Original Article

MOLECULAR BASIS OF ANTI-INFLAMMATORY ACTION OF PLATELET RICH PLASMA ON HUMAN CHONDROCYTES: MECHANISMS OF NF-*k*B INHIBITION VIA HGF

Paola Bendinelli,[1] Emanuela Matteucci,[1] Giada Dogliotti,[1] Massimiliano M. Corsi,[1] Giuseppe Banfi[2,3], Paola Maroni[2] and Maria Alfonsina Desiderio[1*]

[1]Dipartimento di Morfologia Umana e Scienze Biomediche "Città Studi", Molecular and Clinical Pathology Laboratories, Università degli Studi di Milano; [2]Istituto Ortopedico Galeazzi, IRCCS, and [3]Dipartimento di Tecnologie per la Salute, Università degli Studi di Milano, Milano, Italy

*__Correspondence__: Dr. Maria Alfonsina Desiderio, Università degli Studi di Milano, Dipartimento di Morfologia Umana e Scienze Biomediche "Città Studi", Molecular Pathology Laboratory, via Luigi Mangiagalli, 31, 20133 Milan, Italy.

Tel: +39/0250315334; Fax: +39/0250315338; E-mail: a.desiderio@unimi.it

Running head: HGF in PRP inhibitits NF-*k*B

Keywords: HGF, platelet rich plasma, chondrocytes, inflammation, cytokines, NF-*k*B

Number of Tables: 1; **Number of Figures**: 6

Contract grant sponsor: Ministero della Salute; Contract grant number: Ricerca Finalizzata-RF 06-81.

Received 08 February 2010; Revised 12 May 2010; Accepted 03 June 2010

Journal of Cellular Physiology

DOI 10.1002/jcp.22274

Abstract

Loss of articular cartilage through injury or disease presents major clinical challenges also because cartilage has very poor regenerative capacity, giving rise to the development of biological approaches. As autologous blood product, platelet-rich plasma (PRP) provides a promising alternative to surgery by promoting safe and natural healing. Here we tested the possibility that PRP might be effective as an anti-inflammatory agent, providing an attractive basis for regeneration of articular cartilage, and two principal observations were done. First, activated PRP in chondrocytes reduced the transactivating activity of NF-*k*B, critical regulator of the inflammatory process, and decreased the expression of COX2 and CXCR4 target genes. By analyzing a panel of cytokines with different biological significance, in activated PRP we observed increases in hepatocyte growth factor (HGF), interleukin-4 and tumor necrosis factor-α (TNF-α). HGF and TNF-α, by disrupting NF-*k*B-transactivating activity, were important for the anti-inflammatory function of activated PRP. The key molecular mechanisms involved in PRP-inhibitory effects on NF-*k*B activity were for HGF the enhanced cellular IkBα expression, that contributed to NF-*k*B-p65 subunit retention in the cytosol and nucleo-cytoplasmic shuttling, and for TNF-α the p50/50 DNA-binding causing inhibition of target-gene expression. Second, activated PRP in U937-monocytic cells reduced chemotaxis by inhibiting chemokine transactivation and CXCR4-receptor expression, thus possibly controlling local inflammation in cartilage. In conclusion, activated PRP is a promising biological therapeutic agent, as a scaffold in micro-invasive articular cartilage regeneration, not only for its content of proliferative/differentiative growth factors, but also for the presence of anti-inflammatory agents including HGF.

Introduction

Clinical evidence suggests that platelet concentrate could have beneficial therapeutic effects on hard and soft tissue healing, due to the content of growth factors (GFs) stored in the platelets (Lacoste et al., 2003). As autologous blood product, platelet-rich plasma (PRP) provides a promising alternative to surgery by promoting safe and natural healing (Sampson et al., 2008). Recently, we have learned more about specific GFs with a crucial role in healing process. Various GFs are present in PRP: alpha granules are storage units within platelets, which contain pre-packaged GFs in an inactive form. These include platelet-derived growth factor (PDGF), transforming growth factor (TGF)-β1, vascular endothelial growth factor (VEGF) and epidermal growth factor (EGF).

Over the last decade, PRP has found clinical application for the wound healing process in the field of periodontal and oral surgeries, cartilage repair and plastic surgery, and in chronic non-healing musculoskeletal and tendon injuries and cartilage degeneration (Banfi et al., 2006; El-Sharkawy et al., 2007; Sampson et al., 2008; Vardar-Sengul et al., 2009; Cervelli et al., 2009; Pallua et al., 2010; Wu et al., 2009).

Some recent clinical reports suggest that more rapid epithelization, denser and more mature bone with better organized trabeculae, and greater bone regeneration occurred when PRP was added to xenograft and synthetic graft materials (Hanna et al., 2004). As a rich source of GFs, PRP is used in tissue engineering to increase the levels of GFs from intracellular stores potentially maximizing the benefit, as in the case of dental implants and joint space (Tischler, 2002; Sampson et al., 2008).

A lack of post-surgical inflammation is a consistent anecdotal observation associated with the use of PRP (El-Sharkawy et al., 2007). An inflammatory response of appropriate magnitude and timing is crucial for tissue repair and homeostasis (Oberyszyn, 2007). It is imperative, therefore, to develop a novel therapy that could effectively control

inflammation without significant adverse effects for patient safety. Clinical applications and molecular studies with PRP deal with GFs that regulate cellular events such as proliferation, differentiation, chemotaxis and morphogenesis of cells, tissues and organs. However, few studies consider the presence and the possible anti-inflammatory role of cytokines in the PRP after activation with thrombin. Calcium chloride and thrombin may be added to provide a gel matrix for the PRP to adhere to, potentially maximizing the benefit in the case of cartilage repair (Wu et al., 2009). The mechanisms by which thrombin activates platelets and other cells to release various mediators such as GFs have been reviewed (Puri, 1998).

The aim of the present paper was to understand the anti-inflammatory role of cytokines in PRP activated by calcium chloride and thrombin on human chondrocytes, and the molecular mechanism(s) involved. The principal transcription factor regulating the inflammatory process is NF-*k*B, a homo-/hetero-dimer in which subunit association has different biological significances (Perkins, 2006; Ghosh and Hayden, 2008). Dimers containing p65 show transactivating activity. Proteasomal degradation of phosphorylated IkB plays a role in nuclear translocation of p65 subunit of NF-*k*B, regulating transactivating activity, but constitutive NF-*k*B activation is not always associated with increased degradation of IkB. NF-*k*B may be activated by different direct or indirect phosphorylation (Perkins, 2006,) as well as acetylation (Bendinelli et al., 2009). IkBα, considered a gene target of NF-*k*B (Gao et al., 2005), negatively controls transcription factor activity by nucleo-cytoplasmic shuttling of p65 (Arenzana-Seisdedos et al., 1997; Ghosh and Hayden, 2008).

To this purpose, we examined the effects of Hepatocyte growth factor (HGF) and Tumor necrosis factor-α (TNF-α), found augmented in the activated PRP, on the

transactivating activity of NF-*k*B, on the involvement of IkBα in p65 translocation and on the role of the inhibitory p50/50 homodimer in target-gene expression. The molecular mechanisms negatively regulating NF-*k*B activity have never been investigated in chondrocytes exposed to activated PRP. HGF exerts multi-target anti-inflammatory actions (Gong, 2008), and TNF-α elicits a variety of responses, depending on the cellular context (Zetoune et al., 2001). The modulation of NF-*k*B-transactivating activity by autologous-activated PRP in chondrocytes might help to suppress inflammation by inhibiting the expression of pro-inflammatory genes, such as cyclooxygenase-2 (COX-2) (Ulivi et al., 2008). Another mechanism played by activated PRP, involved in limiting local inflammation, seemed to be the prevention of chemotaxis of monocyte-like cells by reducing the expression of chemokine-receptor CXCR4 and the transactivation of chemokines, monocyte chemotactic protein-1 (MCP-1) and RANTES, target genes of NF-*k*B (Nam, 2006).

Materials and Methods

Materials

Recombinant human HGF, interleukin (IL)-4, TNF-α, EGF, VEGF, TGF-β1 and IL-1β as well as human HGF, TGF-β1, PDGF Quantikine immunoassay kits, anti-human CXCR-4-phycoerythrin (PE) (clone 12G5) and IgG_{2A} isotype control-PE antibodies were from R&D System (Abingdon, UK). Thrombin-JMI was from King Pharmaceuticals (Bristol, UK). Anti-IkBα (C21), anti-NF-*k*B p65 (A) and anti-actin antibodies were from Santa Cruz Biotechnology (Santa Cruz, CA). Alexa Fluor 488 and 586 secondary antibodies were from Molecular Probes (Eugene, OR). The gene reporter plasmids NFkBLuc and IkBαLuc were kindly provided by Dr. M. Hung (Anderson Cancer Center, Huston, TX)

and Dr. J. Ye (Luisiana State University System, Baton Rouge, LA); the (-1432/+59)COX-2 gene reporter (COX2Luc) was kindly provided from Dr. S. Wilkinson (Vanderbilt University, Nashville, TN); the original gene reporter pCXCR4(-2632/+86)Luc (kindly provided as pGL2 basic construct by Dr. A. J. Caruz, Universidad de Jaen, Madrid, Spain) was subcloned in the pGL2-enhancer (Maroni et al, 2007); the A20 gene-reporter construct A20-Luc, containing the proximal region of the promoter, was kindly provided by Dr. R. Dikstein (The Weizmann Institute of Science, Rehovot, Israel). MCP-1 (D26087) gene reporter in pGL3-basic was form Dr. I. Morita (Tokyo Madical and Dental University, Tokio, Japan). RANTES gene reporter, containing the promoter spanning -974 to +55, was prepared in pGL3-basic (Pazdrak et al., 2002). The expression vectors for NF-*k*B subunits p50 (pCMV-p50) and p65 (pCMV-p65) were kindly provided by Dr. W.C. Greene (University of California, San Francisco, CA). NK4 to be used *in vitro*, was a gift of Dr. T. Nakamura (University of Osaka, Osaka, Japan).

Cell cultures

The immortalized line of normal human articular chondrocytes (Ibpva55), established by Dr. A. Facchini (Istituti Ortopedici Rizzoli, Bologna, Italy), was used. This line is an ideal model for cartilage research since it represents a permanent and abundant source of cells expressing the physiological characteristics of original tissue (Grigolo et al., 2002). The Ibpva55 cells were cultured in Dulbecco's Modified Eagle's Medium (DMEM) with 25 mM HEPES buffer, 100 U/ml penicillin, 100 µg/ml streptomycin, 50 µg/ml gentamicin, supplemented with 20% foetal bovine serum. The medium was changed twice a week and, at confluence, the cells were trypsinized and expanded in culture (Roseti et al., 2007). Human monocytic tumor cell line U937 was kindly provided by Dr. A. Pessina (University of Milan, Italy). U937 cells were cultured in RPMI-1640 medium

containing 100 U/ml penicillin, 100 µg/ml streptomycin supplemented with 10% foetal bovine serum. All the cells were maintained at 37°C in a humidified atmosphere of 5% CO_2.

Preparation and activation of PRP

Whole-blood samples were collected from 18 healthy donors, undergoing reconstruction of the anterior cruciate ligament, who provided their informed consent. The procedures followed were in accordance with Helsinki Declaration. PRP was obtained using the platelet concentrate collector system GPS II (Biomet, Bridgen, Wales, UK) (Banfi et al., 2006). This system allows the production of PRP with 8-fold concentration of platelets. PRP was activated using 142.8 U/ml thrombin and 14.3 mg/ml $CaCl_2 \cdot 2H_2O$, conditions typically used for clinical application (condition A, reported by Roussy et al., 2007). PRP aliquots were activated for 1 and 24 h at 37°C. Samples were centrifuged for 10 min at 4,000 x g, and PRP supernatants were harvested. Cell count in PRP was made on the smears stained with Giemsa.

Determination of cytokine concentrations in PRP

HGF, PDGF and TGF-β1 were measured in 50 µl of non activated and activated PRP, using Quantikine Immunoassay kits and following manifacturer's protocol. The cytokines IL-4, -6, -8, -10, VEGF, interferon-(IFN-)γ, TNF-α, IL-1α, IL-1β, MCP-1 and EGF were quantified in non activated and activated PRP by a biochip array analyzer (Evidence, Randox Laboratories Ltd, Crumlin, UK). The assay of all 11 molecules was performed simultaneously, using just one assay diluent, one panel-specific conjugate solution and one signal reagent, in 50 µl of non activated PRP and in 5 µl (diluted 1:10 to obtain a final volume of 50 µl) of activated PRP. The biochip used consists of a 9.9-mm solid substrate on which discrete test regions have been constructed. The binding ligands

(antibodies) are attached to predefined sites on the chemically modified surface of the biochip. After a simple enzyme-linked immunoadsorbent assay procedure, the chemiluminescent signals generated at each spot on the array are imaged. The light signal is captured by a charge-coupled device camera as part of an imaging station, and converted by an image-processing software, to provide results compared with calibration curves for each location on the biochip.

Plasmids and cell transfection

For gene reporter assays, NFkBLuc containing three NF-*k*B consensus sequences, IkBαLuc driven by IkBα promoter, COX-2Luc, CXCR4Luc, A20Luc, MCP-1Luc or RANTESLuc promoter construct was used. Adherent (Ibpva55) or suspension (U937) cells, seeded in 24-multiwell plates, were transfected using Fugene 6 (Roche, Basel, Switzerland) (Bendinelli et al., 2009). All these cells were incubated with DNA/Fugene mixture containing 200 ng of each gene reporter per well and 40 ng of pRL-TK (Renilla luciferase) for normalization. Some cells were transfected with 200 ng of the expression vectors for p50 and p65, together with COX-2Luc or A20Luc, or were exposed to 20 ng/ml TNF-α under starvation. Some cells, transfected with the gene reporter, were starved for 16 h and then treated for 24 h with two different volumes (250 or 800 μl) of non activated or activated PRP, or with recombinant human cytokines: HGF (40 ng/ml) (Desiderio et al., 1998), IL-4 (20 ng/ml) (Legitimo et al., 2007), TNF-α (20 ng/ml) (Psarra et al., 2009), EGF (20 ng/ml) (Kim et al., 2009), VEGF (10 ng/ml) (Han et al., 2009), or TGF-β1 (5 ng/ml) (Hiraga et al., 2006). Samples (250 μl) of activated PRP were also tested in the presence of 110 nM NK4 (Kishi et al., 2009). Firefly/*Renilla* luciferase activity ratios were calculated by the software.

Western blot assay

Total extracts (100 μg of proteins) from Ibpva55 cells exposed or not to HGF were examined by Western blot (Bendinelli et al., 2009). β-actin was used for normalization of protein loading. Densitometric analysis was performed after reaction with ECL chemiluminescence kit (GE Healthcare, Milan, Italy).

Immunofluorescence

Ibpva55 cells were seeded (8 x 10^4 per well) on sterile coverslips, previously placed in 24 multiwell plates, and allowed to attach as described (Bendinelli et al., 2009). After starvation for 16 h and treatment with HGF (40 ng/ml for 3 h) or IL-1β (10 ng/ml for 15 min) (Wang et al., 2005), the cells were fixed with 4% paraformaldehyde solution. Slides were then incubated with anti-p65 antibody (1:50), rinsed and probed with the secondary fluorescent antibody Alexa Fluor 568 (1:800). After washing and treatment with paraformaldehyde, reaction with anti-IkBα antibody (1:50) was performed, followed by the secondary fluorescent antibody Alexa Fluor 488. The cells were examined with a fluorescent microscope (Eclipse 80i, Nikon Instruments, Florence, Italy), and the images were collected at X400 magnification.

NF-*k*B-DNA binding activity assay

Protein nuclear extracts were prepared from chondrocytes exposed or not to TNF-α (20 ng/ml for 30 min) with the kit from Active Motif (Carlsbad, CA), and used for binding of NF-*k*B-p50 and p65 subunits to the NF-*k*B consensus sequence 5'-GGGACTTTCC-3'. The measurements were performed with the ELISA-based TransAM-NF-*k*B kit, according to manufacturer's instruction.

Flow cytometry analysis of U937 cells for CXCR4 expression

Starved U937 cells (1.5 X 10^6 cells/well in 6-multiwell plates) were treated overnight with PRP activated for 1h, and were analyzed for CXCR4 expression by flow cytometry

(CyFlow, PAS Partec, Münster, Germany) using anti-human CXCR-4-PE antibody according to the manufacturer's protocol. Isotype-matched IgG_{2A}-PE was used as control.

Chemotaxis assay

Chemotaxis was examined by measuring the migration of U937 cells through a porous membrane (8.0 μm pore size), in response to the CXCR4-agonist CXCL12 and activated PRP, in a 96-well microchamber (NeuroProbe ChemoTx, NeuroProbe Inc. Gaithersburg, MD). In the lower chamber (volume of 300μl), we placed RPMI-1640 without serum supplemented with 100 ng/ml of CXCL12 (Moriuchi et al., 1997) and, when indicated, 250 μl of PRP activated for 1h. Controls without CXCL12 were prepared. Then, 25 μl of U937 cells, suspended to a final concentration of 2 x 10^6 cells/ml in RPMI without serum, were added on the top of the filter for each well. The chambers were incubated for 2 h at 37°C in a humidified incubator. The cells on the upper layer of the membrane were removed with a cotton swab, washing with PBS, and those migrated, adhering to the under side of the filter, were fixed with methanol, stained with Diff-Quick (Dade Behring Inc., Newark, DE), and manually counted under microscope (Eclipse 80i, Nikon Instruments, Florence, Italy) at X400 magnification.

Statistical analysis

All the data were analyzed by analysis of variance, with $P<0.05$ considered significant.

Results

Balance between cytokines with anti-inflammatory significance and pro-inflammatory/proliferative cytokines in activated PRP

Thrombin has been shown to be a potent agent for platelet aggregation and induction of GF and cytokine release (Lacoste et al., 2003). In the present experiments, we activated

PRP with calcium chloride and thrombin, at doses used for clinical applications. PRP activation was performed for short (1 h) and long (24 h) times (Roussy et al., 2007). On average, 8-fold increase in platelet concentration was achieved with GPSII System.

In experiments performed by immunoassay, HGF, TGF-β1 and PDGF concentrations were evaluated under our experimental conditions (Table 1). HGF was present in non activated PRP and increased after activation with thrombin of about 2-4-fold at 1 h and 24 h. It is worth noting that in non activated and activated PRP, HGF had concentrations in the range of ng/ml that might be considered fairly elevated. Both in 1 h- and 24 h-activated PRP, TGF-β1 and PDGF concentrations increased of about 2.5- and 3.5-fold, respectively, when compared with non activated PRP. Further, we observed that monocytes and neutrophils were present in PRP, together with platelets, but they showed a very lower concentration than platelets (Table 1). This finding was consistent with possible HGF production by monocytes and neutrophils (Koyama et al., 2003; Toyama et al., 2005; Gong, 2008), even if the low concentration of monocytes and neutrophils in our PRP samples made difficult to separate them and to evaluate the HGF release.

Then, we measured the concentrations of a panel of cytokines with different biological significance (El-Sharkawy et al., 2007; Sampson et al., 2008; Seruga et al., 2008) (Fig. 1). The activation of PRP for 1 h and 24 h caused remarkable increases in the anti-inflammatory cytokines: IL-4 and IL-10 augmented 11- and 5-fold, respectively. The pro-inflammatory cytokine levels were very low: IL-1β was the most represented and showed a slight increase in the activated PRP, in agreement with the literature (Roussy et al., 2007). Chemotactic factor concentrations were elevated, but did not change in activated PRP. TNF-α increased 2-3-fold at 1 h and 24 h after activation of PRP. The concentration of TNF-α was, however, 1 x 10^2 - to 1 x 10^3 –fold less that those of HGF

and TGF-β1. VEGF and EGF were well represented in non activated PRP, increasing after thrombin exposure, never reaching however the level of HGF.

Inhibition of NF-*k*B transactivatig activity by activated PRP, and role of the various cytokines

To evaluate the possible anti-inflammatory function of PRP, we studied NF-*k*B transactivation using a gene-reporter construct, driven by three NF-*k*B consensus sequences, that was transiently transfected in chondrocytes (Fig. 2A). The measure of luciferase activity, in the case of a gene reporter driven by multiple consensus sequences for a transcription factor, gives a real proof of transcription factor function on gene target expression. We tested two different volumes of non activated and activated PRP. 250 µl of activated PRP reduced of about 60% NF-*k*B transactivation. 800 µl of activated PRP similarly caused 70% decrease of luciferase activity. The inhibitory effect of 250 µl of activated PRP on NF-*k*B transactivation was largely prevented by concomitant treatment of the chondrocytes with NK4, a specific competitive inhibitor of HGF (Kishi et al., 2009).

To clarify which of the GFs and cytokines, increased in activated PRP, were involved in the diminution of NF-*k*B transactivation, HGF, IL-4, TNF-α, VEGF and EGF were tested on NFkBLuc activity (Fig. 2B). HGF alone or in the presence of IL-4 reduced (65%) luciferase activity. IL-4 and TNF-α alone gave inhibitory effects of about 40%. VEGF and EGF were ineffective on NF-*k*B transactivation under our experimental conditions.

The effect of activated PRP in chondrocytes was examined on two NF-*k*B-target genes, COX-2 and CXCR4 expressed in chondrocytes (Maroni et al., 2007; Lee et al., 2008; Ulivi et al., 2008; Haringman et al., 2004), by measuring the luciferase activity of

the gene reporters. Activated PRP reduced of about 50% the COX-2 and CXCR4 luciferase activities (Fig. 2C).

IkBα is involved in the inhibitory effect of HGF on NF-*k*B transactivation in chondrocytes

Some molecular mechanism(s) responsible for NF-*k*B inhibition by HGF were examined by considering the functional role of IkBα in chondrocytes. To this purpose, the luciferase activity of the gene reporter driven by IkBα promoter was measured to evaluate the IkBα gene transcription in chondrocytes. HGF increased (about 2-fold) IkBα luciferase activity (Fig. 3A). Consistently, at 6 and 24 h after HGF treatment IkBα protein level increased (2- 2.5-fold) as shown by Western Blot (Fig. 3B).

The intracellular distribution of endogenous IkBα and p65 after HGF treatment was evaluated by immunofluorescence. As shown in Figure 3C, in starved cells p65 signal was cytoplasmic, and IkBα signal was present in the cytosol and slightly in the nuclei. After HGF exposure, p65 remained in the cytosol and IkBα increased both in the cytosol and nuclei. As shown in merge III, p65 and IkBα signals strongly co-localized in the cytosol after HGF treatment and IkBα was the only signal in nuclei, index of new synthesis (Hochrainer et al., 2007). These molecular events might be related to NF-*k*B activity inhibition. To demonstrate that specific stimuli activating NF-*k*B caused indeed p65 translocation to the nucleus, we treated starved chondrocytes with IL-1β. After treatment with IL-1β, p65 localized prevalently in nuclei while IkBα localization was unchanged, compared to starvation (Fig. 3C).

Role of NF-*k*B-p50 subunit in the TNF-α response in chondrocytes

To clarify the molecular mechanism responsible for inhibition of NF-*k*B transactivation by TNF-α, we used different approaches to study the possible involvement of the p50

inhibitory subunit. It is known that p50 homodimers, that lack transactivation domains, generally repress NF-*k*B-dependent gene expression (Schmitz and Baeuerle, 1991), and p50/50 DNA binding is activated by TNF-α in a pro-inflammatory milieu (Yue et al., 2008).

First, we evaluated the effect of TNF-α treatment on DNA binding of NF-*k*B-p50 or NF-*k*B-p65 subunit. The oligonucleotide used for the binding, furnished by the commercially available kit, has a sequence "GGGACTTTCC", corresponding to the core and the flanking region of NF-*k*B consensus sequence (-223 to -214) present in COX-2 promoter (Chen et al., 2005). As shown in Figure 4A, TNF-α treatment increased of about 6-fold p50-DNA binding, indicating a possible inhibitory role of the homodimer in chondrocytes. p65-DNA binding was only 2-fold higher in TNF-α treated than in starved cells, probably because p50/50 may displace activating p50/65 heterodimers leading to transcriptional repression (Yue et al., 2008).

Then, chondrocytes were transfected with the construct containing the promoter of COX-2 or A20, TNF-α target genes regulated by NF-*k*B (Lee et al., 2008, Li and Lin, 2008). Both TNF-α treatment and p50-expression vector co-transfection inhibited COX-2 and A20 luciferase activities, while the co-transfection with p50 and p65 was ineffective (Fig. 4B).

Endogenous CXCR4 expression in U937 cells was reduced by activated PRP

We hypothesized that activated PRP might control local inflammation in regenerating cartilage not only acting on chondrocyte gene expression, but also by controlling chemotaxis of inflammatory cells. The couple CXCL12/CXCR4 is involved in maintaining homeostatic leukocyte traffic and in the recruitment of monocytes and neutrophils at the sites of inflammation (Haringman et al., 2004). U937 cells are

considered a model for endogenous expression of CXCR4 receptor (Zabel et al., 2009; Moriuchi et al., 1997). In response to overnight exposure to activated PRP, in U937 cells the endogenous expression of CXCR4 was abolished (Fig. 5). This finding is consistent with reduced CXCR4 transactivation observed in chondrocytes exposed to activated PRP, as shown in Figure 2.

Inhibition of CXCL12-induced U937-cell migration by activated PRP

We used the U937-human monocytic tumor cells to evaluate the possible inhibitory role of PRP on chemotaxis of inflammatory cells (Fig. 6).

As shown in Figure 6A, the migration of U937 cells towards CXCL12, the specific CXCR4 ligand, increased 5.5-fold compared to control cells. The latter showed spontaneous migration, and the mean count for ten fields was 40 cells. Migration towards CXCL12 was inhibited by activated PRP from patient 1 (78 %) and from patient 2 (62 %). Representative images of the migrated cells under the different treatments are shown.

Chemokines are a family of pro-inflammatory cytokines that can stimulate the target-cell specific directional migration of leukocytes: MCP-1 and RANTES are produced by monocytes and drive monocyte/macrophage chamotaxis (Julkunen et al., 2001). We transfected MCP-1 and RANTES gene reporters in U937 cells, and the response to activated PRP was studied. As shown in Figure 6B, after exposure to activated PRP the MCP-1 and RANTES luciferase activities were reduced of bout 60 %. To evaluate the possible role of the cytokines present in activated PRP on chemokine expression, the response to TNF-α (20 ng/ml) and TGF-β1 (5 ng/ml) alone or in combination was examined. While TNF-α alone activated MCP-1Luc and RANTESLuc (3.1-fold and 2.3-fold, respectively), TGF-β1 co-treatment largely prevented these activations.

Discussion

In PRP activated by thrombin, at doses used for clinical applications, we found an enhanced content of HGF, IL-4, TNF-α and TGF-β1. We propose that these cytokines participated in the anti-inflammatory effect of activated PRP with various mechanisms: HGF and TNF-α by reducing NF-*k*B transactivating activity and target-gene (COX-2 and CXCR4) expression in chondrocytes, while TGF-β1 counteracted TNF-α effect on chemokine transactivation preventing monocyte chemotaxis. We observed increases in other GFs such as VEGF and EGF, known to regulate angiogenesis like HGF, and also cell differentiation, re-epithelialization and collagenase activity. Enhancement of PDGF might promote granulation tissue formation (Desiderio, 2007; Sampson et al., 2008; Gong, 2008). Pro-inflammatory cytokines were very low in activated PRP. Altogether, these properties of activated PRP, i.e. the control of inflammation and proliferation/differentiation, may have a central role in tissue regeneration (Oberyszyn, 2007).

Activated platelets release TGF-β1, PDGF and VEGF from alpha granules (Roussy et al., 2007), contaminating monocytes and neutrophils are supposed to produce HGF, and leukocytes have an impact on thrombin-induced IL-1β synthesis by platelets (Pillitteri et al., 2007).

Articular cartilage, a specialized connective tissue that bears load and reduces friction across moving joints, has limited regenerative capacity. The treatment of various cartilagineous lesions remains a challenge to clinicians (Wu et al., 2009). Hydrogel, formed by PRP in the presence of thrombin, provides a three-dimensional support to cell growth, and can be used as a scaffold acting as a cell carrier for autologous chondrocyte

implantation into a defective site of articular cartilage (Brehm et al., 2006; Wu et al., 2009). Moreover, autologous PRP is less immunogenic and more biocompatible, than other biomaterials, and is a source of active biological factors, such as HGF. For these reasons we thought interesting to use human chondrocytes as a model.

HGF seemed to exert the anti-inflammatory effect on human chondrocytes through inhibition of NF-*k*B transactivating activity. Most importantly, HGF was the principal cytokine of PRP playing this anti-inflammatory role, because blockade of its function with the specific competitive inhibitor NK4 almost completely prevented the inhibitory effect of activated PRP on NF-*k*B transactivating activity. NK4 is a truncated form of HGF that competes for the binding to Met receptor (Kishi et al., 2009). Our present observations add new data on the role of HGF as potent therapeutic anti-inflammatory agent. It has been reported that HGF inhibits renal inflammation *in vivo*, preventing inflammatory cell infiltration, through disruption of NF-*k*B activity (Giannopoulou et al., 2008).

The key molecular mechanism(s) underlying NF-*k*B inhibitory effect was that HGF impaired p65 translocation to the nucleus, that is necessary for NF-*k*B transactivating activity and gene expression (Perkins, 2006; Ghosh and Hayden, 2008). Under basal conditions, p65 is prevalently localized in the cytosol and p50 is constitutively present in the nuclei (Bendinelli et al., 2009). In response to HGF, IkBα expression increased and possibly contributed to maintain p65 in the cytosol, consistent with the anti-inflammatory role played by IkBα (Wang et al., 2005; Gong, 2008). In addition, when IkBα is increased in the nucleus, as occurred in our experimental conditions after HGF exposure, it might inhibit the interaction of NF-*k*B with DNA

promoting the export of p65 from the nucleus to the cytoplasm (Arenzana-Seisdedos et al., 1997; Ghosh and Hayden, 2008).

The control of the activity of IkBα promoter is complex. Normally, IkBα is considered a NF-*k*B-target gene (Gao et al., 2005). However, other transcription factors are probably involved in the up-regulation of IkBα gene expression, and c-Rel C-terminal may regulate the mRNA level of IkBα by post-transcriptional mechanisms increasing stabilization (Ito et al., 1994; Iwai et al., 2005). In addition, co-activators and co-repressors are simultaneously recruited to the promoter of IkBα. Although different co-repressor complexes, such as SMRT-HDAC1 and NCoR-HDAC3, can inhibit NF-*k*B activity, it seems that they act at different time-points along IkBα transcription induced by NF-*k*B (Gao et al., 2005).

IL-4 and TNF-α might participate in the control of the inflammatory process exerted by HGF in chondrocytes. Because HGF alone or in combination with IL-4, similarly inhibited NF-*k*B transactivating activity, we suggest that the two cytokines shared the signaling pathway activated downstream.

TNF-α was involved in different molecular and cellular events responsible for the control of local inflammatory response, possibly facilitating cartilage healing. First, TNF-α exerted inhibitory effect on COX-2- promoter transactivating activity in chondrocytes, as occurred after exposure to activated PRP. COX-2 is a key pro-inflammatory gene, producing prostaglandin mediators, and is a NF-*k*B-target gene in several cell types including chondrocytes (Alaaeddine et al., 1999; Ulivi et al., 2008; Lee et al., 2008). An important molecular mechanism, accounting for reduction of gene transcription in chondrocytes exposed to TNF-α, seemed to be p50-homodimer formation and its enhanced DNA binding, responsible for the inhibition of NF-*k*B activity. The TNF-α-

induced reduction of A20 expression involved the same mechanism. A20 is a well known inhibitor of NF-*k*B activity, turning-off the TNF-α-activated signal (Li and Lin, 2008). In agreement with the decreased NF-*k*B transactivation by TNF-α in chondrocytes, we observed a remarkable diminution of A20-promoter activity that is dependent on NF-*k*B-activity.

Consistent with our present data, TNF-α decreases the expression of target genes of NF-*k*B by forming homodimers p50/50 in a pro-inflammatory milieu due to activated macrophages that produce TNF-α (Yue et al., 2008). The different responses and the genes regulated by TNF-α may depend on the cellular context, involving specific regulatory mechanisms (Zetoune et al., 2001). We cannot exclude an interaction HGF-TNF-α in chondrocytes exposed to activated PRP, because it is known that HGF attenuates TNF-α-induced phosphorylation of NF-*k*B-p65 subunit and IkBα, and reduces NF-kB-mediated transcriptional activity (Gong et al., 2006). Thus, HGF and TNF-α might contribute to inhibit pro-inflammatory mediators.

Second, activated PRP inhibited monocyte-like cell chemotaxis, possibly by reducing the expression of the chemokine-receptor CXCR4, and of the chemokines MCP-1 and RANTES, all target genes of NF-*k*B (Nam, 2006; Maroni et al., 2007). A possible explanation of the latter inhibitory effect of activated PRP might be that TGF-β1 counteracted the TNF-α dependent stimulation of chemokine transactivating activity. Consistently, negative regulation of mucosal inflammation by TGF-β1 occurs through blockade of TNF-α effect (Stadnicki et al., 2009).

In conclusion, the data herein reported clarify new aspects related to an anti-inflammatory role of activated PRP due to the presence of HGF. These findings are relevant for regenerative medicine because tissue regeneration, including that of cartilage

does not occur without the control of inflammation. Also for periodontal regeneration, PRP facilitates healing by controlling the local inflammatory response (El-Sharkawy et al., 2007). In PRP activated by thrombin at clinical doses not only reparative GFs but also HGF, together with IL-4, TNF-α and TGF-β1, might explain the validity of its application in different clinical fields including micro-invasive articular cartilage regeneration. Our observation that CXCR4 expression was reduced in chondrocytes exposed to activated PRP might have a clinical significance in inflamed synovia, for example by reducing matrix-metalloproteinase secretion, that are cartilage-matrix degrading enzymes.

Acknowledgments

This work was supported by Ministero Salute, Ricerca Finalizzata-RF 06-81.

Literature Cited

Alaaeddine N, Di Battista JA, Pelletier JP, Kiansa K, Cloutier JM, Martel-Pelletier J. 1999. Inhibition of tumor necrosis factor alpha-induced prostaglandin E2 production by the anti-inflammatory cytokines interleukin-4, interleukin-10, and interleukin-13 in osteoarthritic synovial fibroblasts: distinct targeting in the signalling pathways. Arthritis Rheum 42:710-718.

Arenzana-Seisdedos F, Turpin P, Rodriguez M, Thomas D, Hay RT, Virelizier JL, Dargemont C. 1997. Nuclear localization of I kappa B alpha promotes active transport of NF-*k*B from the nucleus to the cytoplasm. J Cell Sci 110:369-378.

Banfi G, Corsi MM, Volpi P. 2006. Could platelet rich plasma have effects on systemic circulating growth factors and cytokine release in orthopedic applications? Br J Sports Med 40:816.

Bendinelli P, Matteucci E, Maroni P, Desiderio MA. 2009. NF-kB activation, dependent on acetylation/deacetylation, contributes to HIF-1 activity and migration of bone metastatic breast carcinoma cells. Mol Cancer Res 7:1328-1341.

Brehm W, Aklin B, Yamashita T, Reiser F, Trüb T, Jakob RP, Mainil-Varlet P. 2006. Repair of superficial osteochondral defects with an autologous scaffold-free cartilage construct in a caprine model: implantation method and short-term results. Osteoarthritis Cartilage 14:1214-1226.

Cervelli V, Palla L, Pascali M, De Angelis B, Curcio BC, Gentile P. 2009. Autologous platelet-rich plasma mixed with purified fat graft in aesthetic plastic surgery. Aesthetic Plast Surg 33:716-721.

Chen J, Zhao M, Rao R, Inoue H, Hao C-M. 2005. C/EBPβ and its binding element are

required for NF*k*B-induced COX2 expression following hypertonic stress. J Biol Chem 280:16354-16359.

Desiderio MA. 2007. Hepatocyte growth factor in invasive growth of carcinomas. Cell Mol Life Sci 64:1341-1354.

Desiderio MA, Pogliaghi G, Dansi P. 1998. Hepatocyte growth factor-induced expression of ornithine decarboxylase, c-met, and c-myc is differently affected by protein kinase inhibitors in human hepatoma cells HepG2. Exp Cell Res 242:401-409.

El-Sharkawy H, Kantarci A, Deady J, Hasturk H, Liu H, Alshahat M, Van Dayke TE. 2007. Platelet-rich plasma: growth factors and pro-and anti-inflammatory properties. J Periodontol 78:661-669.

Gao Z, Chiao P, Zhang X, Lazar MA, Seto E, Young HA, Ye J. 2005. Coactivators and corepressors of NF-*k*B in IkBα gene promoter. J Biol Chem 280:21091-21098.

Ghosh S, Hayden MS. 2008. New regulators of NF-*k*B in inflammation. Nat Rev Immunol 8:837-848.

Giannopoulou M, Dai C, Tan X, Wen X, Michalopoulos GK, Liu Y. 2008. Hepatocyte growth factor exerts its anti-inflammatory action by disrupting nuclear factor-*k*B signalling. Am J Pathol 173:30-41.

Gong R. 2008. Multi-target anti-inflammatory action of hepatocyte growth factor. Curr Opin Investig Drugs 9:1163-1170.

Gong R, Rifai A, Dworkin LD. 2006. Anti-inflammatory effect of hepatocyte growth factor in chronic kidney disease: targeting the inflamed vascular endothelium. J Am Soc Nephrol 17:2464-2473.

Grigolo B, Roseti L, Neri S, Gobbi P, Jensen P, Major EO, Facchini A. 2002. Human articular chondrocytes immortalized by HPV-16 E6 and E7 genes: maintenance of

differentiated phenotype under defined culture conditions. Osteoarthritis Cartilage 10:879-889.

Han KY, Kim CW, Lee TH, Son Y, Kim J. 2009. CCL23 up-regulates expression of KDR/Flk-1 and potentiates VEGF-induced proliferation and migration of human endothelial cells. Biochem Biophys Res Commun 382:124-128.

Hanna R, Trejo PM, Weltman RL. 2004. Treatment of intrabony defects with bovine-derived xenograft alone and in combination with platelet-rich plasma: a randomized clinical trial. J Periodontol 75:1668-1677.

Haringman JJ, Ludikhuize J, Tak PP. 2004. Chemokines in joint disease: the key to inflammation? Ann Rheum Dis 63:1186-1194.

Hiraga T, Myoui A, Choi ME, Yoshikawa H, Yoneda T. 2006. Stimulation of cyclooxygenase-2 expression by bone-derived transforming growth factor-β enhances bone metastases in breast cancer. Cancer Res 66:2067-2073.

Hochrainer K, Racchumi G, Anrather J. 2007. Hypo-phosphorylation leads to nuclear retention of NF-*k*B p65 due to impaired IκBα gene synthesis. FEBS Lett 581:5493-5499.

Ito CY, Kazantsev AG, Baldwin AS Jr. 1994. Three NF-*k*B sites in the IkBα promoter are required for induction of gene expression by TNFα. Nucl Acid Res 22:3787-3792.

Iwai K, Lee BR, Hashiguchi M, Fukushima A, Iwashima M. 2005. IkB-α-specific transcript regulation by the C-terminal end of c-Rel. FEBS Lett 579:141-144.

Julkunen I, Melén K, Nyqvist M, Pirhonen J, Sareneva T, Matikainen S. 2001. Inflammatory responses in influenza A virus infection. Vaccine 19:S32-S37.

Kim S, Choi JH, Lim HI, Lee SK, Kim WW, Cho S, Kim JS, Kim JH, Choe JH, Nam SJ, Lee JE, Yang JH. 2009. EGF-induced MMP-9 expression is mediated by the

JAK3/ERK pathway, but not by the JAK/STAT-3 pathway in a SKBR3 breast cancer cell line. Cell Signal 21:892-898.

Kishi Y, Kuba K, Nakamura T, Wen J, Suzuki Y, Mizuno S, Nukiwa T, Matsumoto K, Nakamura T. 2009. Systemic NK4 gene therapy inhibits tumor growth and metastasis of melanoma and lung carcinoma in syngenic mouse tumor models. Cancer Sci 100:1351-1358.

Koyama T, Hora K, Ako S, Kamijo Y, Higuchi M. 2003. Expression of hepatocyte growth factor is induced by the interaction between human mesangial cells and monocytes. Nephron Exp Nephrol 94:e146-e153.

Lacoste E, Martineau I, Gagnon G. 2003. Platelet concentrates: effects of calcium and thrombin on endothelial cell proliferation and growth factor release. J Periodontol 74:1498-1507.

Lee YH, Suzuki YJ, Griffin AJ, Day RM. 2008. Hepatocyte Growth Factor regulates cyclooxygenase-2 expression via β-catenin, Akt, and p42/44 MAPK in human bronchial epithelial cells. Am J Physiol 294:L778-L786.

Legitimo A, Consolini R, Failli A, Fabiano S, Bencivelli W, Scatena F, Mosca F. 2007. In vitro treatment of monocytes with 8-methoxypsolaren and ultraviolet A light induces dendritic cells with a tolerogenic phenotype. Clin Exp Immunol 148:564-572.

Li H, Lin X. 2008. Positive and negative signaling components involved in TNFα-induced NF-*k*B activation. Cytokine 41:1-8.

Maroni P, Bendinelli P, Matteucci E, Desiderio MA. 2007. HGF induces CXCR4 and CXCL12-mediated tumor invasion through Ets1 and NF-*k*B. Carcinogenesis 28:267-279.

Moriuchi H, Moriuchi M, Arthos J, Hoxie J, Fauci AS. 1997. Promonocytic U937 subclone expressing CD4 and CXCR4 are resistant to infection and cell to cell fusion by T-cell-tropic human immunodeficiency virus type 1. J Virol 71:9664-9671.

Nam NH. 2006. Naturally occurring NF-*k*B inhibitors. Mini Rev Med Chem 6:945-951.

Oberyszyn TM. 2007. Inflammation and wound healing. Front Biosci 12:2993-2999.

Pallua N, Wolter T, Markowicz M. 2010. Platelet rich plasma in burns. Burns 36:4-8.

Pazdrak K, Olszewska-Pazdrak B, Liu T, Takizawa R, Brasier AR, Garofalo RP, Casola A. 2002. MAPK activation is involved in posttranscriptional regulation of RSV-induced RANTES gene expression. Am J Physiol Lung Cell Mol Physiol 283:L364-L372.

Perkins ND. 2006. Post-translational modifications regulating the activity and function of the nuclear factor kappa B pathway. Oncogene 25:6717-6730.

Pillitteri D, Bassus S, Boller K, Mahnel R, Scholz T, Westrup D, Wegert W, Kirchmaier CM. 2007. Thrombin-induced interleukin 1beta synthesis in platelet suspensions: impact of contaminating leukocytes. Platelets 18:119-127.

Psarra AM, Hermann S, Panayotou G, Spyrou G. 2009. Interaction of mitochondrial thioredoxin with glucocorticoid receptor and NF-*k*B modulates glucocorticoid receptor and NF-*k*B signalling in HEK-293 cells. Biochem J 422:521-531.

Puri RN. 1998. Phospholipase A2: its role in ADP-and thrombin-induced platelet activation mechanisms. Int J Biochem Cell Biol 30:1107-1122.

Roseti L, Facchini A, De Franceschi L, Marconi E, Major EO, Grigolo B. 2007. Induction of original phenotype of human immortalized chondrocytes: a quantitative gene expression analysis. Int J Mol Med 19:89-96.

Roussy Y, Duchesne MPB, Gagnon G. 2007. Activation of human platelet-rich plasma: effect on growth factor release, cell division and in vivo bone formation. Clin Oral Impl Res 18:639-648.

Sampson S, Gerhardt M, Mandelbaum B. 2008. Platelet rich plasma injection grafts for musculoskeletal injuries: a review. Curr Rev Musculoskelet Med 1:165-174.

Schmitz ML, Baeuerle PA. 1991. The p65 subunit is responsible for the strong transcription activating potential of NF-*k*B. EMBO J 10:3805-3817.

Seruga B, Zhang H, Bernstein LJ, Tannock IF. 2008. Cytokines and their relationship to the symptoms and outcome of cancer. Nat Rev Cancer 8:887-899.

Stadnicki A, Mechnik G, Klimacka-Nawrot E, Wolanska-Karut A, Labuzek K. 2009. Transforming growth factor-β1 and its receptors in patients with ulcerative colitis. Int Immunopharmacol 9:761-766.

Tischler M. 2002. Platelet rich plasma. The use of autologous growth factors to enhance bone and soft tissue grafts. NY State Dent J 68:22-24.

Toyama T, Ido A, Sasak H, Maeda K, Yamashita K, Kubiki Y, Suzuki M, Matsuoka H, Tsubouchi H. 2005. Possible involvement of neutrophils in a serum level increase of hepatocyte growth factor in non-Hodgkin's lymphoma. Oncol Rep 13:439-444.

Ulivi V, Giannoni P, Gentili C, Cancedda R, Descalzi F. 2008. p38/NF-kB-dependent expression of COX-2 during differentiation and inflammatory response of chondrocytes. J Cell Biochem 104:1393-1406.

Vardar-Sengul S, Arora S, Baylas H, Mercola D. 2009. Expression profile of human gingival fibroblasts induced by interleukin-1β reveals central role of nuclear factor-kappa B in stabilizing human gingival fibroblasts during inflammation. J Periodontol 80:833-849.

Wang W, Huang XR, Li AG, Liu F, Li J-H, Truong LD, Wang XJ, Lan HY. 2005. Signaling mechanism of TGF-β1 in prevention of renal inflammation: role of Smad 7. J Am Soc Nephrol 16:1371-1383.

Wu W, Zhang J, Dong Q, Liu Y, Mao T, Chen F. 2009. Platelet-rich plasma - A promising cell carrier for micro-invasive articular cartilage repair. Med Hyp 72:455-457.

Yue L, Christman JW, Mazzone T. 2008. Tumor necrosis factor-α-mediated suppression of adipocytes apolipoprotein E gene transcription: primary role for the nuclear factor (NF)-*k*B pathway and NF-*k*B p50. Endocrinology 149:4051-4058.

Zabel BA, Wang Y, Lewén S, Berahovich RD, Penfold MET, Zhang P, Powers J, Summers BC, Miao Z, Zhao B, Jalili A, Janowska-Wieczorek A, Jaen JC, Schall TJ. 2009. Elucidation of CXCR7-mediating signaling events and inhibition of CXCR4-mediated tumor cell transendothelial migration by CXCR7 ligands. J Immunol 183:3204-3211.

Zetoune FS, Murthy AR, Shao Z, Haling T, Zeildler MG, LiY, Vincenz C. 2001. A20 inhibits NF-*k*B activation downstream of multiple MAP3 kinases and interacts with IkB signalosome. Cytokine 15:282-298.

Legends to figures

Fig. 1. Mean concentrations of a panel of cytokines and growth factors in PRP from 9 patients. The data are the mean ± S.E. of experiments repeated three times. □ Non-activated PRP; PRP activated for ▒ 1 h and ■ 24 h. *P<0.05, **P<0.005 and ***P<0.001 vs. non-activated PRP.

Fig. 2. Activated PRP was responsible for inhibition of NF-*k*B-transactivating activity, as well as of CXCR4 and COX-2 target genes. **A:** Chondrocytes transfected with the construct containing the NFkB multimer, were treated with non-activated (n.a.) PRP or activated (a.) PRP, in the presence or the absence of 110 nM NK4. The histograms indicate the absolute values for Firefly/*Renilla* luciferase activity ratios. Columns, mean of five independent experiments (5 patients) performed in triplicate; bars, S.E. *P<0.05 and **P<0.005 vs. n.a. PRP (250 µl); $^{\Delta}$P<0.05 vs. n.a. PRP (800 µl); $^{\circ}$ P<0.05 vs. a. PRP (250 µl). **B:** Chondrocytes transfected with the construct containing the NFkB multimer, were treated with the various cytokines and growth factors shown. The histograms indicate the absolute values for Firefly/*Renilla* luciferase activity ratios. Columns, mean of three independent experiments performed in triplicate; bars, S.E. *P<0.05 and **P<0.005 vs. starved (st) cells. **C:** Chondrocytes transfected with COX-2 or CXCR4 gene reporter, were treated with 250 µl of a. PRP or n.a. PRP. The histograms indicate the absolute values for Firefly/*Renilla* luciferase activity ratios. Columns, mean of two independent experiments (2 patients) performed in triplicate; bars, S.E. **P<0.005 vs. untreated-gene reporter transfected cells.

Fig. 3. Expression of IkBα after HGF treatment. **A:** Chondrocytes were transfected with IkBα promoter and exposed to HGF. The histograms indicate the absolute values for Firefly/*Renilla* luciferase activity ratios. Columns, mean of three independent experiments performed in triplicate; bars, S.E. *P<0.05 vs. st cells. **B:** Western blot analysis carried out with total protein extracts from cells exposed or not to HGF. Anti-β-actin antibody was used for normalization. The numbers at the bottom indicate the fold-variations relative to the starvation value, considered as 1. The experiments have been repeated three times with similar results. **C:** Immunofluorescence images of chondrocytes treated with HGF or IL-1β and probed with anti-p65 and anti-IkBα antibodies. The nuclei were stained with DAPI (bleu). Merge I, p65/DAPI; merge II, IkBα/DAPI; merge III, p65/IkBα. The images, taken at X400 magnification, are representative of experiments performed in triplicate.

Fig. 4. Role played by NF-*k*B-p50 subunit in the inhibitory response to TNF-α. **A:** The chondrocytes were treated with TNF-α, and 10 µg nuclear protein extracts were used for DNA binding of p50 or p65. The histograms indicate the fold-increase of DNA binding in TNF-α treated vs. untreated cells, considered as 1. Columns, mean of three independent experiments performed in triplicate; bars, S.E. *P<0.05 and **P<0.005 vs. st-untreated cells. **B:** Chondrocytes transfected with COX-2Luc or A20Luc, were treated with TNF-α or were co-transfected with p50 in combination or not with p65 expression vector. The histograms indicate the absolute values for Firefly/*Renilla* luciferase activity ratios. Columns, mean of three independent experiments performed in triplicate; bars, S.E. *P<0.05 and **P<0.005 vs st cells transfected with the gene reporter (COX-2Luc or A20Luc).

Fig. 5. CXCR4 expression in U937 cells exposed to activated PRP (a. PRP) or in untreated control cells assessed by flow cytometric analysis. **A:** Starved U937 cells, treated overnight with a. PRP (500 µl), were stained with an isotype control antibody (grey area) or the monoclonal anti-CXCR4 antibody, and were analyzed by flow cytometry. Two independent experiments (2 patients) were performed, and the determinations were repeated three times with similar results. Representative images are shown. **B:** Columns show the percentage of positive cells, reacting with anti-CXCR4 antibody, after subtraction of the aspecific (isotype-antibody reaction) area. The data are the mean ± S.E. of two independent experiments repeated three times. ***P<0.001 vs. control cells.

Fig. 6. Activated PRP reduced the monocyte migration induced by CXCL12. **A:** Chemotaxis assay of U937 cells was performed for 2 h towards starvation medium (control cells, C) or towards CXCL12, in the presence or the absence of activated PRP (250 µl) from two patients (P1 and P2). The data shown are the mean ± S.E. of two independent experiments performed in triplicate, using the cell count of ten fields/well. When the bars indicating S.E. are not shown, they are within the column. ***P < 0.001 vs. control cells; $^{\Delta\Delta}$ P < 0.005 vs. CXCL12-exposed cells. Representative light microscopy images of Diff-Quik-stained U937 cells are shown (X400 magnification). **(B)** U937 cells were transfected with the gene reporter constructs for MCP-1 and RANTES, in the presence or the absence of activated PRP (250 µl) from two patients, or were treated with TNF-α and TGF-β1 alone or in combination. The histograms indicate the absolute values for Firefly/*Renilla* luciferase activity ratios. Columns: mean of

experiments carried out with PRP from 2 patients, and performed in triplicate; for TNF-α and TGF-β1 mean of two independent experiments performed in triplicate; bars, S.E. When the bars indicating S.E. are not shown, they are within the column. *P < 0.05 and **P < 0.005 vs. control cells; $^{\Delta}$P<0.05 and $^{\Delta\Delta}$P < 0.005 vs. TNF-α-treated cells.

Table 1

Concentration of HGF in non activated and activated PRP

PRP	HGF (ng/ml)	Fold increase
Non activated	2.28 ± 0.22	
Activated 1h	4.14 ± 0.39*	1.8
Activated 24h	8.19 ± 0.79**	3.6

Number of patients = 5. *P<0.05; **P<0.005.

Concentrations of TGF-β1 and PDGF in non activated and activated PRP

PRP	TGF-β1 (ng/ml)	Fold increase	PDGF (ng/ml)	Fold increase
Non activated	12.42 ± 1.31		3.15 ± 0.45	
Activated 1h	32.81 ± 4.55**	2.6	11.34 ± 1.95**	3.6
Activated 24h	31.27 ± 4.03**	2.5	10.71 ± 1.63**	3.4

Number of patients = 5. **P <0.005

Cell count of platelets, monocytes and neutrophils in PRP

Cell type	10^6 cells/ml
Platelets	1,850 ± 320
Monocytes	2.5 ± 0.6
Neutrophils	3.2 ± 0.9

Number of patients = 5.

Fig.1

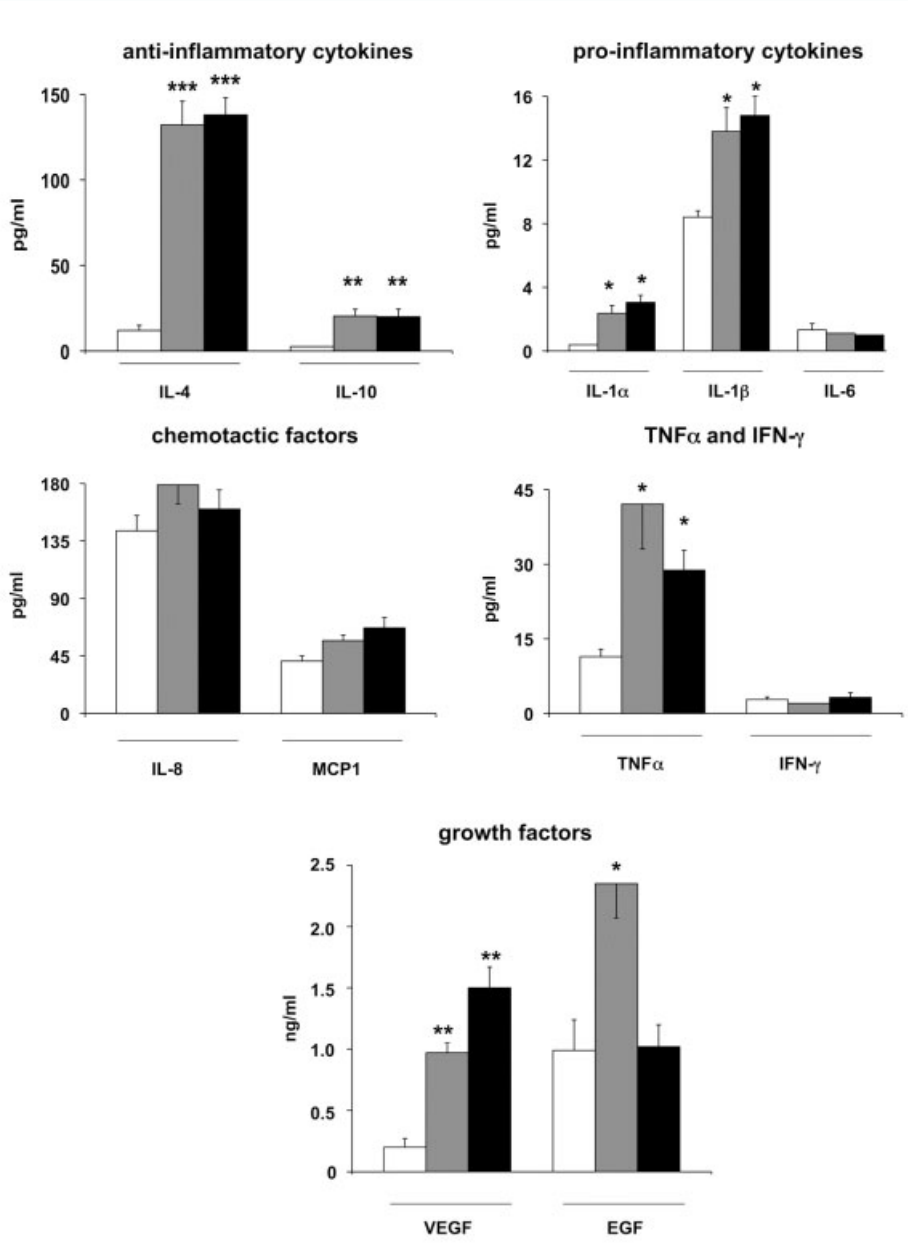

Fig.2

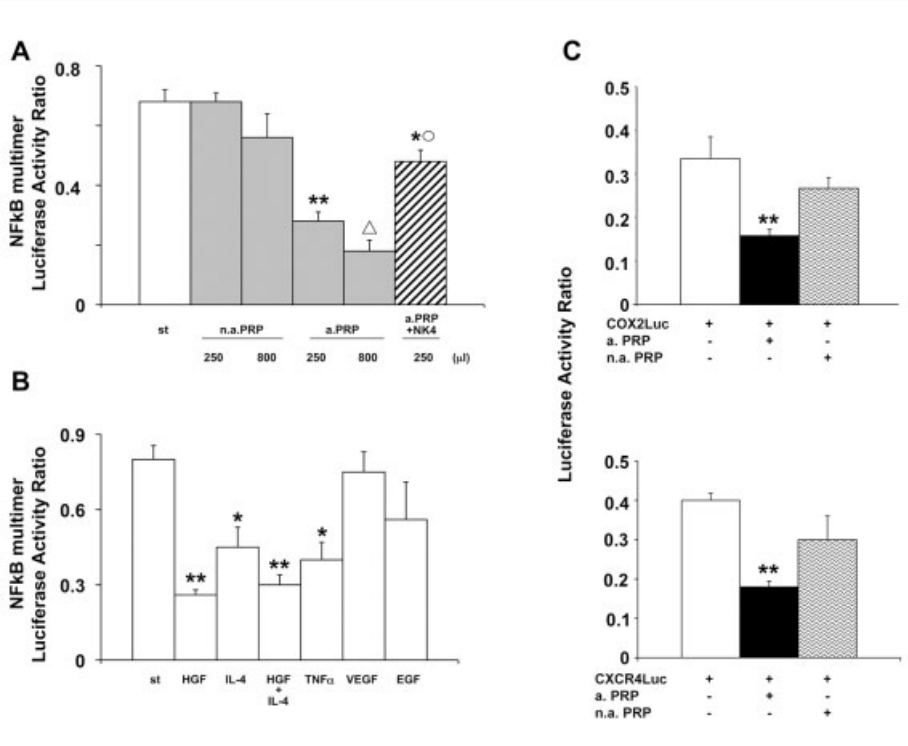

Fig.3

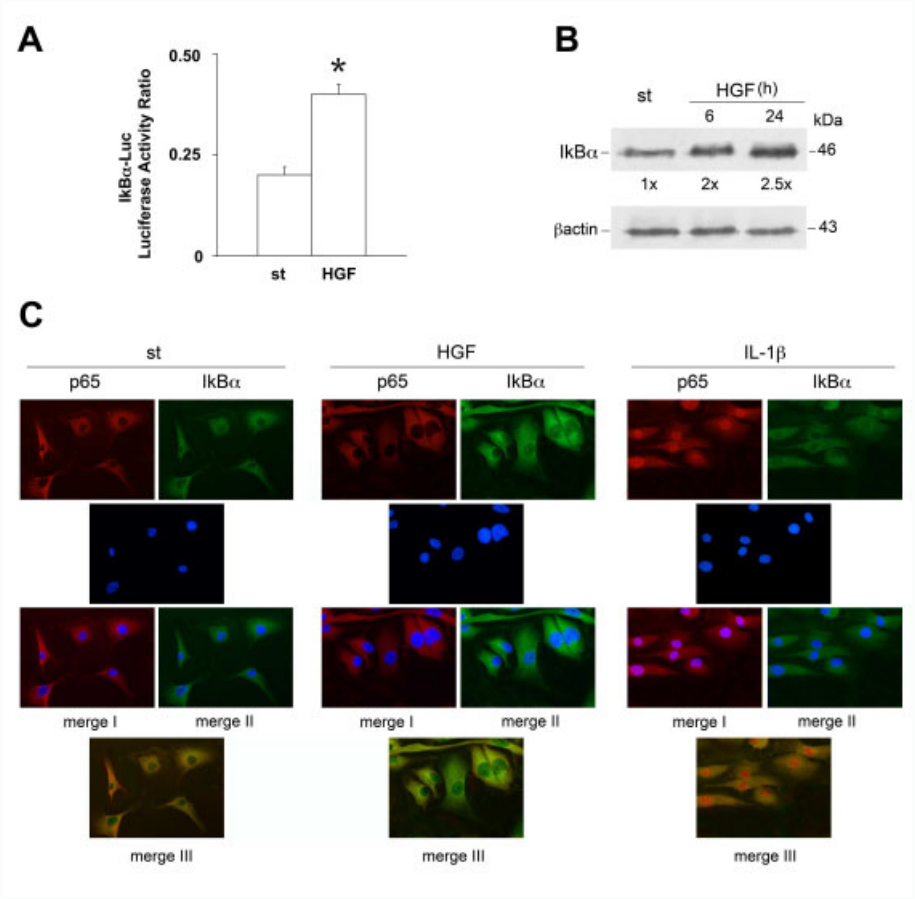

Fig.4

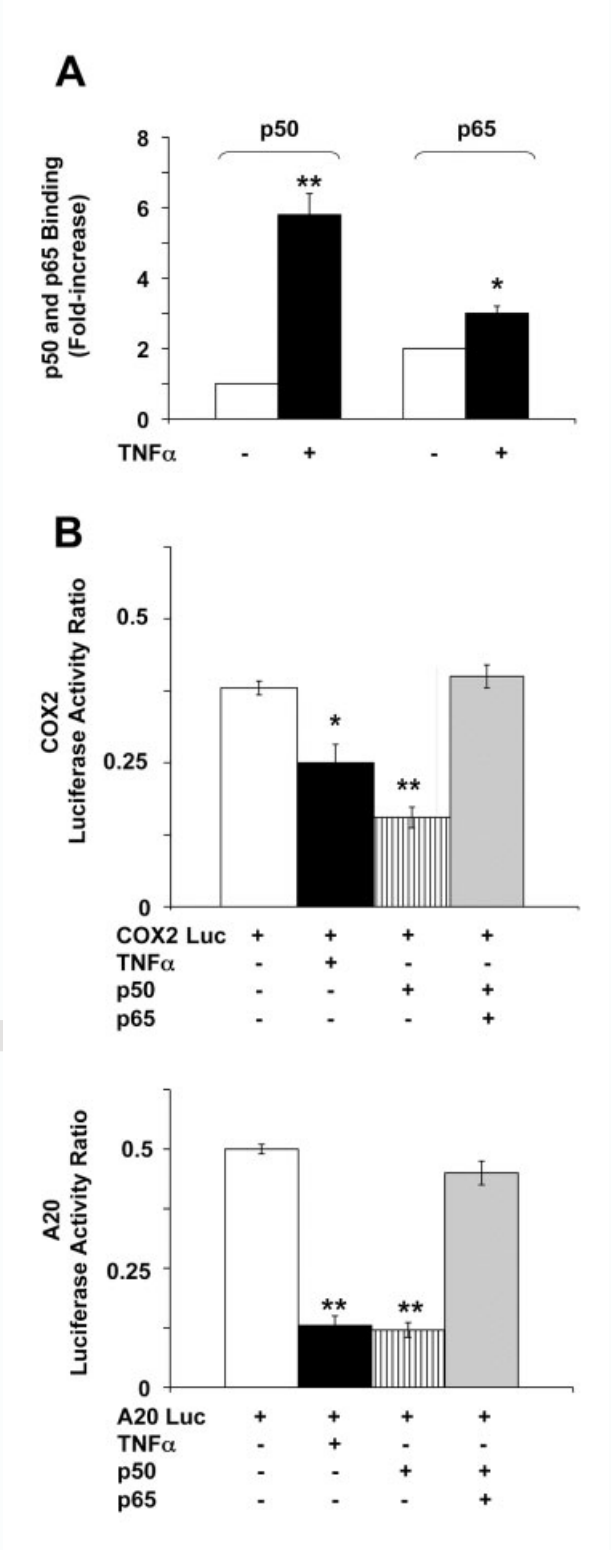

Fig.5

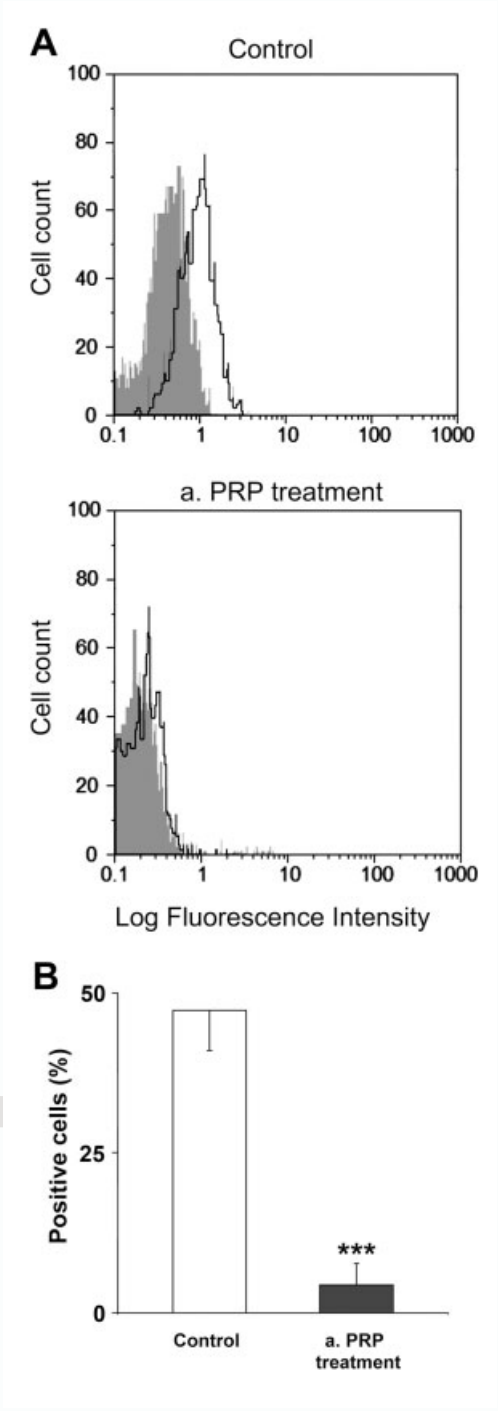

Fig.6